JOURNAL OF GEOPHYSICAL RESEARCH, VOL. 97, NO. B13, PAGES 19,791–19,801, DECEMBER 10, 1992

Thermodynamic and Anharmonic Properties of Forsterite, α-Mg_2SiO_4: Computer Modelling Versus High-Pressure and High-Temperature Measurements

BRUNO REYNARD[1] AND GEOFFREY D. PRICE

Department of Geological Sciences, University College London,London, England

PHILIPPE GILLET[2]

Laboratoire de Minéralogie Physique, Geosciences Rennes, Université de Rennes, Rennes, France

Self-consistent minimum free-energy calculations of the structure and lattice dynamics of forsterite at high pressure (up to 30 GPa) and high temperature (up to 1850 K) have been performed using an approach based on the Born model of solids. In the free-energy minimization procedure, lattice dynamics and thermodynamic properties are calculated self-consistently within the quasi-harmonic approximation (QHA). The results of the free-energy minimizations are compared with recent spectroscopic studies of forsterite at high pressure and high temperature. The predicted variations of mode frequencies with compression are consistent with those obtained from high-pressure spectroscopy. On the other hand, the variations with temperature are underestimated. Because the variations of lattice dynamics with pressure are related to anharmonic properties such as the Gruneisen parameter and thermal expansion, it is concluded that most of the extrinsic (i.e., volume dependent) anharmonicity can be accounted for within the QHA. On the other hand, the variations of the lattice dynamics with temperature also include intrinsic (i.e., volume free) anharmonic effects, which are not accounted for in the QHA. In forsterite, these effects become significant for thermodynamic properties (heat capacities and thermal expansion) above 1200 K.

INTRODUCTION

Accurate mineralogical and compositional modeling of the Earth's mantle from seismic data requires the knowledge of the thermodynamic properties of minerals at the very high pressures and temperatures that they experience in the Earth's interiors. In particular, equations of state are needed to model the observed density and sound velocity profiles, while thermal and anharmonic properties are needed to infer the temperature gradient and predict phase relations.

With the development of high pressure apparati, the in situ study of minerals under mantle conditions has become possible. Specifically, equations of state can be established from, for instance, X ray diffraction; on the other hand, the determination of thermodynamic properties (entropies and high-temperature heat capacities) of high-pressure phases is less straightforward because of the minute amounts available and because they are metastable at ambient pressure and high temperature. The estimation of thermodynamic properties is generally achieved through the vibrational modeling of spectroscopic IR and Raman data at ambient [*Kieffer*, 1979a, b, c, 1980, 1982; *Akaogi et al.*, 1984] or high pressure [e.g., *Chopelas*, 1990a, b]. In vibrational modeling, however, the quasi-harmonic approximation (QHA) is often assumed. Recent calorimetric and spectroscopic studies of forsterite α-Mg_2SiO_4 and its germanate analogues Ca_2GeO_4 and Mg_2GeO_4 [*Gillet et al.*, 1989, 1991; *Fiquet et al.*, 1992] have shown that, as expected, the QHA breaks down at high temperature.

In parallel with experimental investigations, various methods for the computer modeling of mineral structures and properties have been derived from different approximations of the fundamental theory of quantum mechanics, or from empirical atomistic models [e.g., *Catti*, 1986; *Cohen*, 1987; *Dovesi et al.*, 1987; *Wolf and Bukowinski*, 1987; *Catlow and Price*, 1990]. They have proved successful in predicting the properties or stability fields of candidate mantle minerals. However, in order to keep computer time within reasonable limits, the thermal and anharmonic properties have to be obtained through the calculation of lattice dynamics within the QHA.

Finally, in the interpretation of seismic data [*Anderson*, 1987, 1989] or in the calculation of the adiabatic gradient [*Stacey*, 1977; *Brown and Shankland*, 1985; *Quareni and Mulargia*, 1989], the QHA is often assumed, on the grounds that anharmonic effects are limited to high temperatures and low pressures [*Hardy*, 1980]. Thus it is essential to define the conditions for which anharmonicity can be neglected, i.e., where the QHA is valid.

Because anharmonicity has been extensively studied in forsterite [e.g., *Anderson and Suzuki*, 1983; *Gillet et al.*, 1991], we have performed minimum free-energy calculations on this mineral at simulated high temperature and high pressure, using a Born-Mayer atomistic model of solids [*Born and Huang*, 1954]. The calculation of lattice dynamics was performed within the QHA and compared with high pressure-high temperature IR and Raman spectroscopic results in order to discuss the limits of the QHA.

[1]Now at Laboratoire de Minéralogie Physique, Géosciences Rennes, Université de Rennes I, Rennes, France.

[2]Now at Laboratoire de Géologie, Ecole Normale Supérieure de Lyon, Lyon, France.

Paper number 92JB01554.
0148-0227/92/92JB-01554 $05.00

THE ATOMISTIC MODEL

We use an approach based upon the Born model of solids in which the interaction between atoms is described by a potential of the form [*Born and Huang*, 1954]:

$$U=\sum_{ij}(e^2q_iq_jr_{ij}^{-1} + A_{ij}exp(-r_{ij}/B_{ij}) - C_{ij}r_{ij}^{-6}) \quad (1)$$

where the first term describes the coulombic interaction (with e the electron charge, q_i and q_j the point charges associated with the ions i and j, and r_{ij} the distance between them), and the second term the short range interaction (where A_{ij}, B_{ij} and C_{ij} are derivable constants). In order to model the directionality of the Si-O bonds, a bond bending term is included in the potential:

$$U = \sum_{ijk} k^B_{ijk}(\theta_{ijk}-\theta_0)^2 \quad (2)$$

where k^B_{ijk} is a derivable spring constant, θ_{ijk} is the O-Si-O bond angle and θ_0 the ideal tetrahedral angle of 109°47'. Finally, the polarizability of the oxygen is modeled by a core-shell interaction, where a massless shell of charge Y is coupled to the core containing all the mass by a harmonic spring:

$$U = \sum_i k_S r_i^2 \quad (3)$$

where k_S is the constant of the spring and r_i the core-shell separation.

For the THB1 potential used in this study (Table 1), the parameters were derived from fitting either to quantum mechanic energy surfaces or to the structural and elastic properties of binary oxides [*Price et al.*, 1987a]. The structural, elastic and thermodynamic properties (in association with lattice dynamics) are then calculated at various simulated pressures and temperatures using energy minimization procedures available via the code PARAPOCS [*Parker and Price*, 1989]. THB1 has been found successful in modeling the structure, lattice dynamics and thermodynamics of forsterite and its high-pressure polymorphs [*Price et al.*, 1987a, b].

TABLE 1. The THB1 Potential Set (Short Range Cutoff 10Å)

Potential Constant	Value
q_{Mg}	+2.0
q_{Si}	+4.0
$q_{O\text{-}shell}$	-2.848
$q_{O\text{-}core}$	+0.848
k_S eVÅ^{-2}	74.92
k^B eVrad^{-2}	2.09
$A_{Mg\text{-}O}$ eV	1428.5
$A_{Si\text{-}O}$ eV	1283.9
$A_{O\text{-}O}$ eV	22764.3
$B_{Mg\text{-}O}$ Å	0.2945
$B_{Si\text{-}O}$ Å	0.3205
$B_{O\text{-}O}$ Å	0.1490
$C_{O\text{-}O}$ eVÅ^6	27.88
$C_{Si\text{-}O}$ eVÅ^6	10.66

TABLE 2. Predicted and Measured Properties of Forsterite at P=0 and T=300 K

	V, Å^3	K_T, GPa	α, 10^{-5} K^{-1}	αK_T, 10^{-3} GPa K^{-1}	γ,
Calculated	296.1	150.4[a]	1.89[a]	2.84[a]	1.09[a]
		142.6[b]	2.00[b]	2.82[b]	1.09[b]
Observed	289.9	127.4	2.72	3.45	1.29

Experimental values from *Isaak et al.* [1989].

[a] Properties from the self-consistent energy-minimization procedure, neglecting the derivatives of the thermal pressure.

[b] Properties obtained from the predicted volumes at high pressures and high temperatures.

COMPUTED EQUATION OF STATE OF FORSTERITE

The TBH1 predicted structure and elastic properties of forsterite at ambient conditions (Table 2) have been extensively discussed by *Price et al.* [1987a]. A third-order Birch-Murnaghan equation of state was fitted to the calculated volumes at high pressure and 300 K, yielding K_{T0} = 142.6 GPa and $K'_0 \approx 4.15$, in agreement within 10% with ultrasonic measurements [*Graham and Barsch*, 1969; *Kumazawa and Anderson*, 1969; *Suzuki et al.*, 1983; *Isaak et al.*, 1989]. The pressure derivative of K_{T0} is also close to K'_0 = 4.65 obtained from ultrasonic measurements on olivine up to 3 GPa [*Webb*, 1989]. The model also predicts the decrease of K'_0 with increasing pressure observed by this author, if a polynomial fit is used. The predicted value decreases to $K'_0 \approx 2.5$ at 30 GPa, in good agreement with the average values of ~3.5 derived from shock experiments covering the same pressure range [*Syono and Goto*, 1982; *Brown et al.*, 1987]. There is thus good evidence that the derivative of the bulk modulus of olivine compounds decreases with pressure, although it is commonly assumed to be constant to derive equations of state from, for instance, X ray measurements.

Similarly, the thermal expansion is derived from the calculated volumes at high temperature. We obtain a value of 2.0 10^{-5} K^{-1} at 300 K, 20 to 30% lower than the experimental value of 2.5-2.8 10^{-5} K^{-1} [*Suzuki*, 1975; *Hazen*, 1976; *Suzuki et al.*, 1983; *Anderson and Suzuki*, 1983; *Takeuchi et al.*, 1984; *Matsui and Manghnani*, 1985; *White et al.*, 1985; *Isaak et al.*, 1989]. For internal consistency throughout this paper, we use the experimental high-temperature values of K_T, α, and other anharmonic properties (Gruneisen and Anderson-Gruneisen parameters) from *Isaak et al.* [1989] in the comparison with computed properties. Detailed discussion of the uncertainties associated with the different experimental determinations of the thermal expansion of forsterite was given by *Isaak et al.* [1989] and *Gillet et al.* [1991].

AMBIENT CONDITION LATTICE DYNAMICS AND MODE ASSIGNMENT

Assignment of the calculated (q=0)-frequencies is straightforward since the PARAPOCS code not only gives the eigenvalues of the dynamical matrix, i.e., the frequencies, but also the eigenvectors, i.e., the associated atomic motions. The calculated frequencies are in overall good agreement with single-crystal IR and Raman spectroscopic investigations

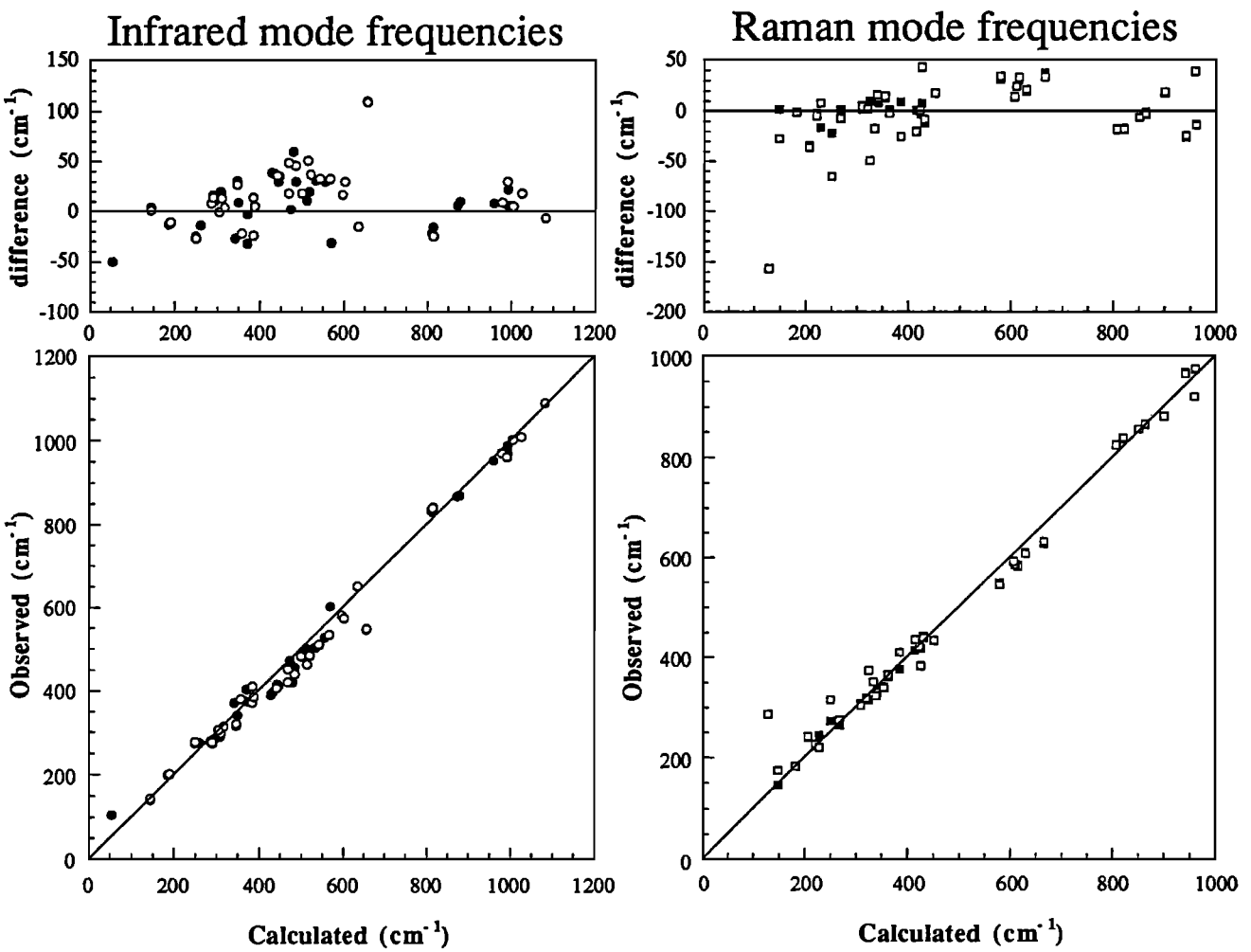

Fig. 1. Predicted versus observed vibrational (q=0)-frequencies, in wavenumbers. Raman experimental data from *Iishi* [1978] (solid symbols) and *Chopelas* [1991] (open symbols). Infrared experimental data from *Reynard* [1991], solid symbols for tranverse frequencies, open for longitudinal. Also reported the lowest frequency Au mode experimental value from inelastic neutron scattering [*Rao et al.*, 1988]. 1:1 line reported for reference. Absolute differences between calculated and observed frequencies are plotted.

[*Price et al.*, 1987a] (Figure 1), and we hereinafter use the correspondance proposed in Table 3 between calculated and observed frequencies. However, a few frequencies are predicted incorrectly, due to intrinsic shortcomings in the potential. For these modes, discrepancies can be as large as 50 to 150 cm^{-1}, indicating incorrect prediction of the eigenvectors. In particular, low-frequency modes (i.e. external modes) are the most sensitive to the errors in the predicted atomic motions because of the low force constants and large structural distorsions for the octahedra when compared with the tetrahedra. Transverse-longitudinal infrared mode frequency splitting are correctly predicted, especially for the high-frequency modes (800-1100 cm^{-1}) which are clearly resolved in most IR reflectance spectra [*Servoin and Piriou*, 1973; *Iishi*, 1978; *Reynard*, 1991]. This shows that the polarizability of ions in the structure is reasonably accounted for by the core-shell interaction. A greater discrepancy is obtained if infrared data from *Hofmeister* [1987] are used for the comparison but this is mainly related to several polarization mixing problems in this study as discussed by *Reynard* [1991]. Other discrepancies of a few wavenumbers between the different studies can be explained by the different samples, spectral resolutions and theoretical analysis methods that were used: these small discrepancies do not affect the present comparison. Finally, several infrared modes have not yet been unambiguously observed.

We wish to emphasize that the computed lattice dynamics are obtained from the empirical potential THB1 that has been fitted only to the structural and elastic properties of oxides at ambient conditions, not to the observed Raman and IR frequencies. It yields, however, results that are very similar to a recent pair potential [*Lam et al.*, 1990] fitted to the experimental vibrational data. Because THB1 has 11 adjustable parameters and because it is able to reproduce the TO-LO splitting of IR modes, we prefer it, in spite of its shortcomings, to the more complicated potential used by *Lam et al.* [1990] which has 19 adjustable parameters and does not account for the dielectric properties.

LATTICE DYNAMICS AT HIGH PRESSURES

Experimental Results

Several investigations of the spectroscopic properties of forsterite at high pressure have been recently performed, and they include both Raman [*Besson et al.*, 1982; *Gillet et al.*, 1988,1991; *Chopelas*, 1990b] and IR studies [*Dietrich and*

TABLE 3. Predicted and Observed Mode Frequencies and Gruneisen Parameters

Theoretical		Observed			Theoretical		Observed	
ν_i	γ_i	$\nu_i^{a(b)}$	γ_{iT}^{c}	γ_{iP}^{d}	ν_i	γ_i	ν_i^{e}	γ_{iT}^{f}
A_g					A_u			
182	1.64	183(183)	2.09	2.51	55	5.78	105	-
221	0.43	223(226)	0.67	1.82	167	-0.87	-	-
309	1.89	307(304)	1.63	2.87	248	1.35	-	-
342	0.98	334(329)	1.16	2.18	270	0.72	-	-
354	2.45	341(339)	1.87	2.82	336	1.54	-	-
423	1.50	426(422)	1.43	1.62	387	1.13	-	-
579	0.16	548(545)	0.53	0.77	448	0.60	-	-
629	0.41	610(608)	0.70	0.82	477	0.60	-	-
806	0.25	825(824)	0.48	0.79	517	0.61	-	-
850	0.30	856(856)	0.49	0.72	937	0.24	-	-
941	0.33	967(965)	0.66	1.07				
B_{1g}					B_{1u}			
228	1.42	244(220)	1.21	2.13	175-176	0.76	-	-
267	1.31	265(274)	-	-	249-250	1.03	274-277	-
320	2.20	316(318)	-	-	309-317	1.44	289-313	1.25
334	1.10	-(351)	-	-	343-358	1.21	370-380	-
426	0.50	418(383)	-	-	371-386	1.61	403-410	-
452	1.00	434(434)	1.40	-	446-469	1.14	411-451	-
615	0.41	585(582)	0.66	0.85	474-500	0.65	472-482	-
665	0.43	628(632)	-	-	512-597	0.37	501-580	-
820	0.22	837(838)	-	-	879-1026	0.26	869-1008	0.39
863	0.34	864(866)	-	-				
961	0.32	974(975)	-	-	B_{2u}			
					144-144	2.15	140-143	1.52
B_{2g}					261-286	1.71	275-278	1.69
148	1.05	146(175)	-	-	294-304	1.59	283-305	1.47
206	0.30	240(242)	-	-	350-385	1.74	341-371	0.85
339	2.59	324(323)	-	-	429-442	0.81	390-406	-
363	0.78	361(365)	-	-	445-485	0.96	415-439	0.65
431	1.07	443(439)	1.60	2.52	486-521	0.71	456-484	0.58
610	0.19	586(586)	-	-	534-543	0.80	503-510	-
900	0.25	882(881)	0.40	1.00	556-603	0.42	526-573	0.88
					669-670	0.33	-	-
B_{3g}					814-816	0.23	830-841	0.44
129	4.30	-(286)	-	-	873-979	0.26	867-970	0.30
250	0.14	272(315)	-	-	993-1006	0.35	987-1001	0.79
325	0.89	315(374)	-	-				
385	1.75	376(410)	1.25	1.94	B_{3u}			
415	0.85	414(435)	0.99	2.04	186-190	2.30	199-201	1.91
606	0.27	593(592)	-	0.85	290-290	1.16	274-276	1.37
959	0.23	920(920)	0.38	0.82	306-310	1.20	289-297	
					347-347	0.61	316-320	1.23
					371-389	1.45	374-384	-
					435-469	0.78	397-420	-
					480-514	0.46	420-463	-
					518-567	0.67	498-534	-
					570-635	0.51	601-650	0.39
					656-657	0.25	546-548	-
					811-814	0.22	833-839	-
					960-991	0.22	952-961	-
					993-1082	0.24	971-1089	-

Predicted frequencies calculated at T=300 K and P=0 (against T=0 and P=0 of *Price et al.* [1987a]).

[a] *Iishi* [1978].

[b] *Chopelas* [1991].

[c] *Chopelas* [1990b].

[d] *Gillet et al.* [1991].

[e] *Reynard* [1991] except the frequency of the A_u mode from inelastic neutron scaterring [*Rao et al.*, 1988].

[f] *Hofmeister et al.* [1989].

Arndt, 1982; *Hofmeister et al.*, 1989].

High-pressure Raman spectroscopy. We use the data collected by *Chopelas* [1990b] on 19 modes up to 18 GPa, which are mostly comparable with the other studies [*Besson et al.*, 1982; *Gillet et al.*, 1988, 1991] but which cover a wider pressure range and number of modes with a higher resolution. Below about 9 GPa, the pressure dependence of the mode frequencies is linear within the experimental uncertainties. Above this pressure, the bands exhibit three different types of behavior: (1) some weaken and quickly disappear as pressure is increased, (2) some present a lower dependence of frequency upon pressure and (3) some still present the same pressure dependence (high-frequency internal modes). The inferred mode Gruneisen parameters :

$$\gamma_{iT} = -(\partial \ln \nu_i / \partial \ln V)_T = K_T / \nu_i (\partial \nu_i / \partial P)_T \quad (4)$$

are lower for the internal modes than for the lattice modes. The decrease of the $(\partial \nu_i / \partial P)_T$ slope for some modes above 9 GPa leads to a decrease in their γ_{iT}. This is observed not only for the low-frequency (external) modes but also for the bending and one stretching mode of the silicon tetrahedron. However, the change in slope is lower for the internal modes than for the lattice modes.

High-pressure IR spectroscopy. Infrared data [*Hofmeister et al.*, 1989] were collected up to 45 GPa from both single- and poly-crystalline samples. The IR modes behave like the Raman modes: (1) a nearly linear frequency dependence on pressure up to about 10 GPa, (2) above 10 GPa, some modes (in the range 200-450 cm^{-1}) exhibit a smooth slope decrease, (3) some weaken and disappear, and (4) some (mainly internal modes) show no change in behavior. The mode Gruneisen parameters are similar to those of the Raman modes, i.e., low for the internal modes of SiO_4 and high for the lattice modes. The mode Gruneisen parameters decrease with pressure for those modes which exhibit a strong negative curvature in their ν_i versus P relationship. In contrast with the Raman data, such a behavior is not observed for the internal modes.

Computer Modeling

The pressure dependence of the (q=0)-frequencies of the 81 optic modes of forsterite have been calculated up to 30 GPa. The results are plotted in Figure 2 along with the experimental results. The agreement between data and calculations is good. This is also revealed by the similar values of the predicted and observed mode Gruneisen parameters (Table 3, Figure 3). The main discrepancy comes from the γ_{iT} values of the internal modes of the silicon tetrahedron which are systematically lower from theory (0.15 to 1.5 with an arithmetic mean of 0.42) than from experiments (0.3 to 1.6 with an arithmetic mean of 0.66); this is probably due to the high predicted incompressibility of the SiO_4 tetrahedron (≈550 GPa), which is more than twice the value commonly derived from high-pressure X ray refinements for orthosilicates [*Hazen and Finger*, 1982, 1989; *Kudoh and Takeuchi*, 1985]. The high predicted imcompressibility of the tetrahedron has little influence on the bulk modulus because the compression of the structure is mainly governed by the octahedra. The predicted mode Gruneisen parameters of the external modes are in good overall agreement with experiments (-0.9 to 5.8 with an arithmetic mean about 1.37 against 0.6 to 2.1 with an arithmetic mean about 1.33, respectively). The wider scatter of values from theory may be due to the fact that some eigenvectors are incorrectly predicted; in particular, the values predicted for low-frequency modes (50 to 150 cm^{-1}) are generally high (4 to 6) because γ_{iT} values are inversely proportional to the mode frequency. Similarly, the negative value for one A_u mode Gruneisen parameter is dubious, although negative shifts with pressure are observed in some compounds such as rutile, tetragonal GeO_2 and stishovite [*Mammone and Sharma*, 1979; *Hemley*, 1987; *Sharma*, 1989]. In experiments, these modes cannot be observed either because they are spectroscopically inactive (A_u symmetry) or because they are too weak. In high-pressure infrared studies, for instance, spectra are collected over an area were pressure gradient are large, causing a broadening of the peaks that may impede the resolution of small peaks located near strong peaks. In contrast, high-frequency internal modes, which are the more intense in both vibrational spectroscopies, are more evenly sampled in high-pressure measurements (21 for 33 IR and Raman active plus 3 inactive). However, only a few values are inconsistent with available experimental data and do not have a significant effect on the average values, which are quite similar.

The frequency versus pressure relation for the internal stretching modes is nearly linear (very slight slope decrease) as observed in both Raman and IR studies. Significant slope decrease with increasing pressure is predicted for low-frequency modes (100-400 cm^{-1}), in agreement with both Raman and IR high-pressure data. On the other hand, slight slope increase is typically predicted for modes at about 400-500 cm^{-1} as well as for bending internal modes. The predicted slope variations in the frequency versus pressure relation are consistent with those observed in vibrational data at high pressure. The predicted variations can be complicated (inflection points) which means that there is no theoretical need to fit vibrational data with straight lines, especially when slope changes can be observed. In particular, fitting different parts of one curve with lines of different slope rather than a continuous polynomial function might lead to inaccurate description of the frequency evolution with pressure. Using linear fits, *Chopelas* [1990b] has suggested that the change in the vibrational properties of forsterite above 9 GPa might be related to some reversible phase transition. Such a transition is not predicted from the model. Thus confirmation of its existence by other techniques (e.g. X ray diffraction) is required before definitive conclusions can be drawn. Moreover, the uncertainties associated with the spectroscopic measurements probably impede the resolution of most subtle details such as the ones predicted (e.g., slight slope increase for bending modes), although curvature in the Raman mode frequency evolution with pressure was observed, for instance, in quartz [*Hemley*, 1987].

LATTICE DYNAMICS AT HIGH TEMPERATURE

Experimental Results

Raman spectra of forsterite have been collected up to 1350 K by *Gillet et al.* [1991]. Within the experimental temperature range and uncertainties, the frequencies display a linear negative dependence on temperature. In order to compare these results with the high-pressure data, it is necessary to define a dimensionless parameter, the isobaric Gruneisen parameter [*Mammone and Sharma*, 1979], as:

$$\gamma_{iP} = -(\partial \ln \nu_i / \partial \ln T)_P = -(1/\alpha \nu_i)(\partial \nu_i / \partial T)_P \quad (5)$$

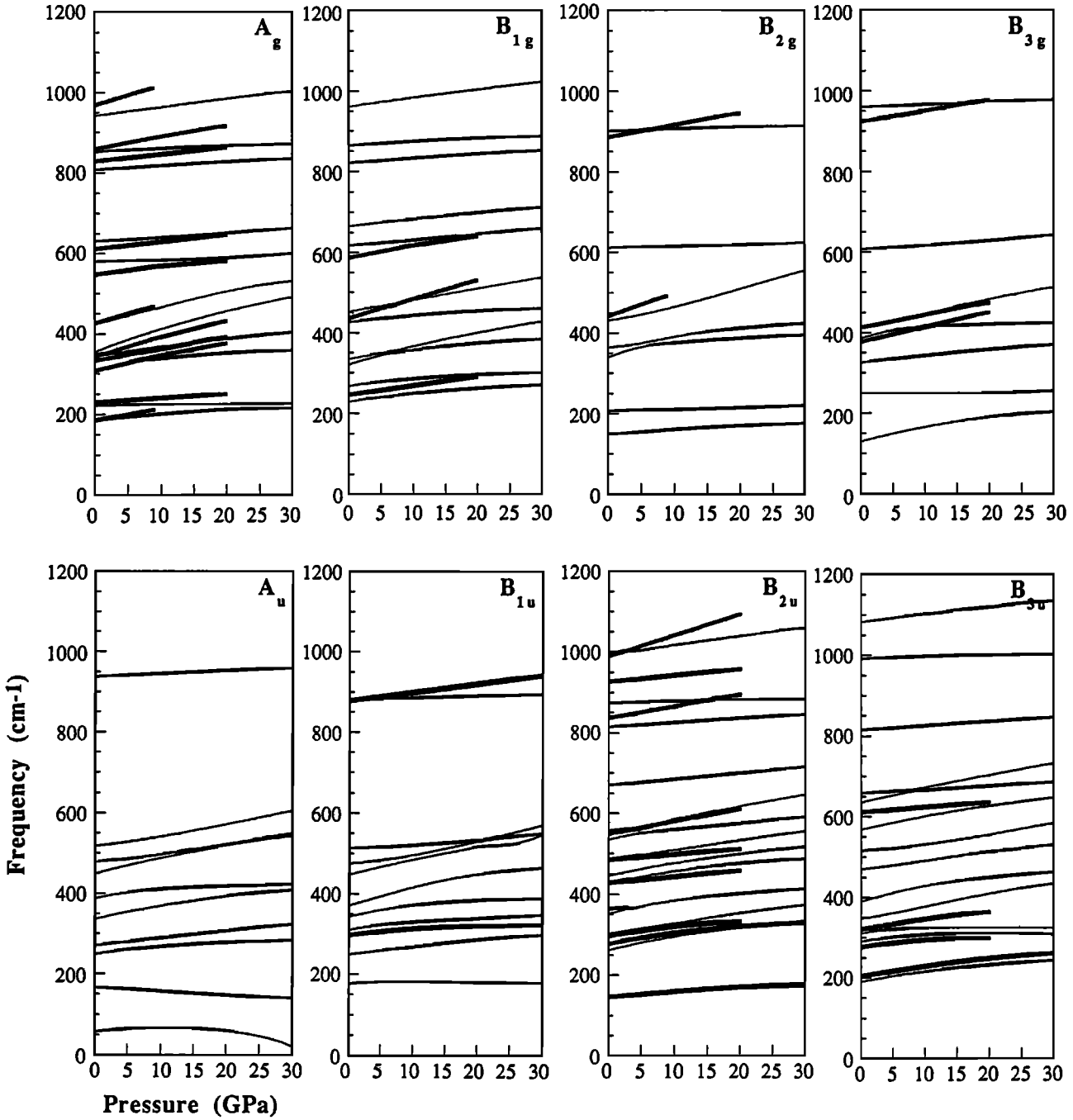

Fig. 2. Predicted (thin lines) and observed (thick lines) (q=0)-frequency shifts with pressure. Raman data from *Chopelas* [1990b]. IR data from *Hofmeister et al.* [1989]. Predicted frequencies for q = 0.001, 0, 0 (transverse B_{1u} and B_{2u} and longitudinal B_{3u}).

These are found to be in general significantly different and higher than the classical isothermal ones (Table 3). This difference has been shown to be a measure of intrinsic mode anharmonicity [*Mammone and Sharma*, 1979; *Gillet et al.*, 1989] through an anharmonic mode parameter defined as:

$$a_i = (\partial \ln \nu_i / \partial T)V = \alpha(\gamma_{iT} - \gamma_{iP}) \quad (6)$$

For a harmonic mode, $\gamma_{iT} = \gamma_{iP} = a_i = 0$; for a quasi-harmonic mode, $\gamma_{iT} = \gamma_{iP} \neq 0$ and $a_i = 0$; for an anharmonic mode, $\gamma_{iT} \neq \gamma_{iP}$ and $a_i \neq 0$ [*Gillet et al.*, 1989]. Because the measured isobaric parameters are in general higher than isothermal ones, the a_i parameters are usually negative, indicating significant mode anharmonicity.

Computer Modeling

As a result of the QHA used in the energy minimization procedure, intrinsic anharmonic effects are not accounted for. Thus we do not find any difference between the calculated isothermal and isobaric mode Gruneisen parameters. The computed frequency variations with temperature (Figure 4) and

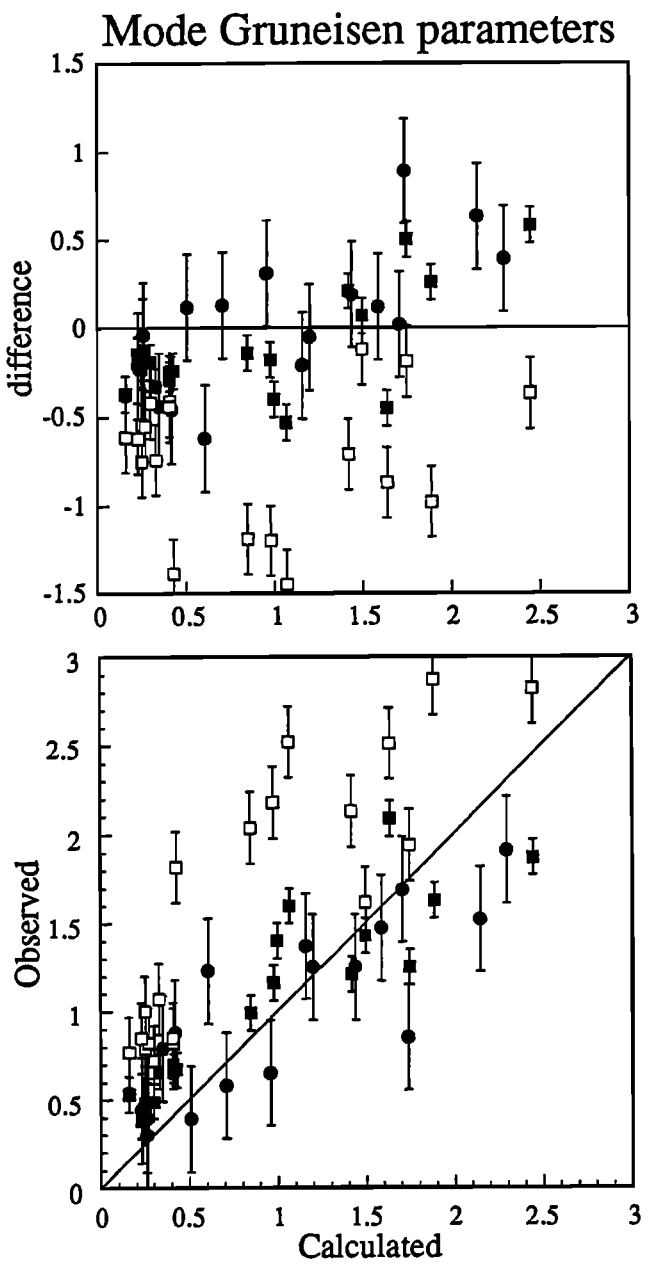

Fig. 3. Predicted and observed mode Gruneisen parameters. Squares : Raman modes; circles : IR modes. Solid symbols: γ_{iT}, open symbols: γ_{iP}. The overall good agreement between calculated and observed γ_{iT} values is marked by the scatter of points about the 1:1 correlation line. On the contrary, the predicted γ_{iP} values are in general too low and all representative points above the 1:1 line. Also, absolute differences between calculated and measured are all negative for the γ_{iP} values whereas they are scattered around the zero line for the γ_{iT} values.

γ_{iP} are very different from the actual ones (Table 3, Figure 3) and the observed frequency shifts with temperature are reproduced only qualitatively.

MODE GRUNEISEN, MACROSCOPIC GRUNEISEN PARAMETERS AND THERMAL EXPANSION

Mode Gruneisen and Anharmonic Parameters

Before discussing the relationships between the mode Gruneisen, γ_i, and the macroscopic Gruneisen, γ, parameters,

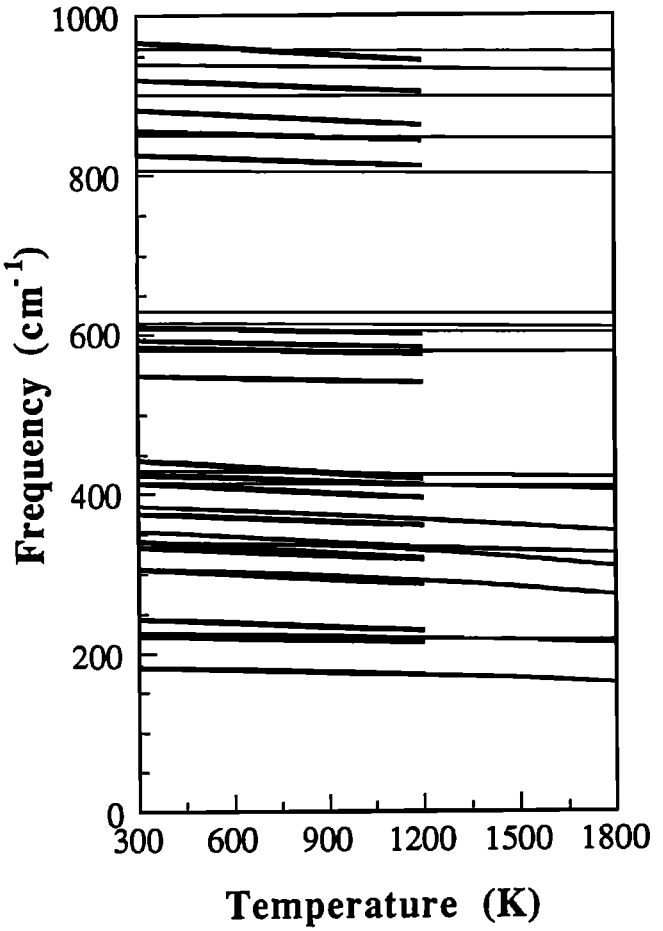

Fig. 4. Predicted (thin lines) and observed (thick lines) (q=0)-frequency shifts with temperature. Only Raman modes that have been measured and the corresponding calculated values are plotted. Raman data from *Gillet et al.* [1991].

several conclusions concerning the predicted mode Gruneisen parameters must be outlined: (1) the computed γ_{iT} values are in overall good agreement with the observed ones; (2) the computed γ_{iP} values are equal to the γ_{iT} values because the QHA is assumed in the free-energy minimization; on the other hand, the observed γ_{iP} values are in general significantly higher than the γ_{iT} values, indicating a significant contribution from intrinsic anharmonic effects; (3) the predicted γ_i values for the internal modes are significantly lower than for external modes as was observed from spectroscopic measurements.

As a consequence of the QHA, the computed a_i parameters are equal to zero ($\gamma_{iT} = \gamma_{iP}$). The difference between the measured γ_{iT} and γ_{iP} leads to actual values of the a_i values of forsterite significantly different from zero. Nevertheless, the good agreement between the computed and measured γ_{iT} values implies that the intrinsic (or constant-volume) anharmonic contribution is mainly related to the γ_{iP} values. Consequently, most of the extrinsic part of anharmonicity (Gruneisen parameter and thermal expansion) can be accounted for within the QHA.

Macroscopic Gruneisen Parameter

The macroscopic Gruneisen parameter of a mineral can be calculated from its bulk elastic and thermodynamic properties

as:

$$\gamma_{th} = \alpha K_T V/C_V = \alpha K_S V/C_P \quad (7)$$

where γ_{th} is the thermal Gruneisen parameter.

Its definition was introduced by *Gruneisen* [1912] from the microscopic parameters of the vibrational modes $\gamma_{iT} = (\partial \ln \nu_i/\partial \ln V)_T$, in a crystal where all γ_{iT} are equal to the macroscopic γ. In the case where the γ_{iT} are different, it can be shown that within the QHA [e.g., *Cochran*, 1973]:

$$\gamma_{th} = \langle\gamma\rangle = \Sigma C_{Vi}\gamma_{iT}/C_V \quad (8)$$

where C_{Vi} is the contribution of the ith mode to the heat capacity at constant volume, and $\langle\gamma\rangle$ the mean Gruneisen parameter, which can thus be regarded as the quasi-harmonic macroscopic parameter.

In the present study the thermal Gruneisen is obtained from this latter relation [*Price et al.*, 1987b] and used to calculate the thermal expansion from (8). Indeed, the predicted $\langle\gamma\rangle$ (1.09) is lower by ~20% than the thermal one (1.29) calculated from the bulk properties of forsterite [*Isaak et al.*, 1989] (Table 2) but close to the mean Gruneisen parameter (~1.1-1.2) obtained from the frequency shifts of Raman and IR bands at high pressure [*Hofmeister et al.*, 1989; *Chopelas*, 1990b]. The predicted mean Gruneisen parameter is thus close to the measured ones. The difference between the measured mean and thermal Gruneisen parameters is also observed for other minerals such as pyroxenes, spinel or periclase [*Chopelas*, 1990a, b, c, personal communication, 1989; *Gillet et al.*, 1991] and orthogermanates [*Gillet et al.*, 1989; *Fiquet et al.*, 1992]. This is not surprizing since it has been shown from combined high-pressure and high-temperature spectroscopic measurements and calorimetry that intrinsic anharmonic effects are significant in these compounds [*Gillet et al.*, 1989; *Richet and Fiquet*, 1991]. *Gillet et al.* [1991] have shown how intrinsic anharmonicity can be accounted for in the derivation of the macroscopic Gruneisen parameter from microscopic data, and obtain:

$$\gamma_{th} = \Sigma \gamma_{iT} C_{Vi}/C_V + \Sigma \gamma_{iT} a_i (U_i^h - TC_{Vi})/C_V + \Sigma (\partial \gamma_{iT}/\partial T)_V U_i^h \quad (9)$$

where U_i^h is the harmonic contribution of the ith mode to the internal energy, and C_V is the heat capacity including intrinsic anharmonic contributions. In the QHA, the two last terms are equal to zero which yields equation (8). However, this simple intrinsic anharmonic correction does not resolve all the differences between the spectroscopic and the thermal Gruneisen parameters, especially at high temperatures. *Gillet et al.* [1991] attribute the large discrepancy at high temperature to the last term of the right-hand side of equation (9), or to the increase of the γ_{iT} values with temperature which cannot be evaluated from the available data. The present calculation indicate an overall increase of the γ_{iT} values with temperature and would support this latter interpretation, but intrinsic anharmonicity could counterbalance this effect. Other factors which could resolve these discrepancies include the possible dispersion of the Gruneisen parameters across the Brillouin zone. Such a dispersion effect is expected in anisotropic solids where a tensorial definition of the generalized Gruneisen parameters can be established in relation to the Lagrangian strains [*Leibfried and Ludwig*, 1960] and has been demonstrated in MgO from high-pressure fluorescence measurements [*Chopelas*, 1990a]. In our energy minimization, the mode and average Gruneisen parameters were calculated at 27 points in the Brillouin zone (BZ) and the $\langle\gamma\rangle$ quoted in Table 2 is the average over the whole BZ. The values of the individual $\langle\gamma\rangle$ at the 27 points in the BZ are scattered from 1.05 to 1.31. The value at the center of the BZ (i.e. the spectroscopic one) is 1.23 (as compared with 1.19 calculated from spectroscopic data with equation (8)), and significantly higher than the mean value of 1.09. This difference is thus of the order of magnitude of the discrepancy between the spectroscopic $(q=0)\langle\gamma\rangle$ and thermal γ, but would bring the $\langle\gamma\rangle$ to even lower values.

Whatever the case, the different shortcomings and assumptions in the calculation of mean Gruneisen parameters from spectroscopic data lead to inaccuracies of the order of about 15%, which is the common scatter of values used, for instance, in the calculation of adiabatic gradients [*Quareni and Mulargia*, 1988, 1989]. The values obtained with the quasi-harmonic modeling are lower than the measured thermal Gruneisen parameters by about the same order of magnitude.

Thermal Expansion

In the free-energy minimization, the thermal expansion is calculated self-consistently from equation (8) :

$$\alpha = \langle\gamma\rangle C_V/K_T V \quad (10)$$

The theoretical value at 300 K is 20 to 30% lower than the actual one (Table 2). The discrepancy comes from two sources: (1) the overestimation of the bulk modulus in the model (10%) and, (2) the underestimation of the Gruneisen parameter as discussed previously. However, the shape of the relative change of thermal expansion with temperature is well predicted up to 1300K (Figure 5), i.e. a strong increase up to 700K then a linear increase of α. Above this temperature, the predicted variations are strongly overestimated because intrinsic anharmonic effects become very important at such

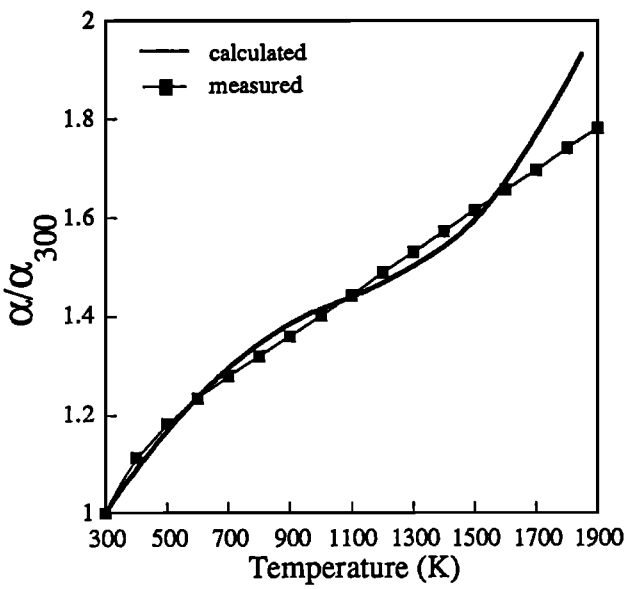

Fig. 5. Predicted and observed relative variations of thermal expansion with temperature. Experimental data from Kajiyoshi, quoted by *Isaak et al.* [1989].

temperatures. Above 1850K, the energy minimization fails because of the breakdown of the QHA.

DISCUSSION AND CONCLUSIONS

Using the THB1 potential to investigate the lattice dynamics of forsterite at high pressure and high temperature, we find that on the one hand, the variations of the predicted (q=0)-phonon frequencies with pressure compare favorably with both Raman and IR investigations up to 30 GPa, while on the other hand, the variations with temperature are not quantitatively predicted.

The disagreement with the high-temperature data is attributed to intrinsic anharmonic effects which cannot be modeled within the QHA used in the free-energy minimization. Inversely, the good agreement with high-pressure data shows that most of the extrinsic, i.e., volume dependent properties such as the Gruneisen parameter and related thermal expansion can be modeled within the QHA.

Therefore the QHA proves useful in predicting the thermodynamic properties of minerals provided that within the P-T range of interest, the intrinsic anharmonic effects are negligible. *Hardy* [1980] has shown qualitatively that anharmonic effects are restricted to relatively high temperatures and low pressures and might therefore be neglected in most studies of the mantle. However, it is highly desirable to have a more quantitative estimate of the extent of anharmonic effects for mineral phases relevant to the mantle. The analysis of the properties of forsterite is probably the best way to constrain these effects because they have been extensively characterized.

Recent studies [*Gillet et al.*, 1989, 1991; *Fiquet et al.*, 1992] on forsterite and its analogues (Ca_2GeO_4, Mg_2GeO_4) have shown that intrinsic anharmonic effects on thermodynamic properties, such as the heat capacity, become significant above 1200 to 1500 K at ambient pressure. In particular, the heat capacity at constant volume exceeds the harmonic Dulong and Petit (DP) limit (3R J atom^{-1} K^{-1}), which is diagnostic of the occurrence of significative anharmonicity (Figure 6). In order to investigate whether such effects persist at high pressure, we can write the isothermal relative variations of the constant volume heat capacity with volume from equation (8) as [*Anderson and Yamamoto*, 1987]:

$$(\partial \ln C_V/\partial \ln V)_T = (\partial \ln \alpha/\partial \ln V)_T + (\partial \ln K_T/\partial \ln V)_T + (\partial \ln V/\partial \ln V)_T - (\partial \ln \gamma/\partial \ln V)_T = \delta_T - K' + 1 - q \quad (11)$$

where $\delta_T = (\partial \ln \alpha/\partial \ln V)_T$ is the Anderson-Gruneisen parameter and $q = (\partial \ln \gamma/\partial \ln V)_T$ the second Gruneisen parameter. In the temperature range were anharmonic effects are significant (T>1200K), the QHA yields values of C_V close to the DP limit and nearly independent of volume at constant temperature. We thus have $(\partial \ln C_V/\partial \ln V)_T \approx 0$, consistent with the computed values of $\delta_T \approx 6.5$, $K' \approx 4.0$ and $q \approx 3.5$. The theoretical value of δ_T compares favorably with the experimental value of 5.4±0.5 [*Isaak et al.*, 1989] and the predicted K' is nearly insensitive to temperature as commonly assumed in high-temperature equations of state. On the other hand, the predicted q is high when compared with the values of 1 to 2 estimated from, for instance, adiabatic measurements [*Boehler*, 1982]. This is due, in first order, to the overestimation by ≈ 1 of δ_T and the underestimation by ≈ 0.5 of K', i.e., to the inherant shortcoming of the model, and possibly to intrinsic anharmonic effects. Recent calculations based with the QHA on MgO, using a more sophisticated potential [*Isaak et al.*, 1990], led to an almost perfect agreement with experiment for these second-order parameters. If we now try to estimate the isothermal relative variations of the constant volume heat capacity with volume from the experimental values of δ_T, K' and q, we obtain $(\partial \ln C_V/\partial \ln V)_T \approx 0.3 \pm 1.5$ (assuming that K' is constant with temperature). Thus the experiments tend to indicate that C_V is nearly independent of pressure at constant temperature but the uncertainties associated to the second-order parameters preclude definitive interpretation.

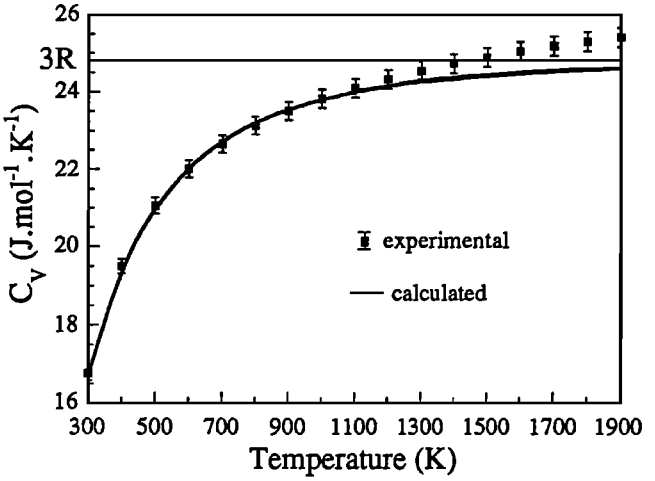

Fig. 6. Predicted variations of C_V (thin line) with temperature at ambient pressure versus experimental data from *Robie et al.* [1982] and *Gillet et al.* [1991]. The harmonic Dulong and Petit limit (3R) also reported for comparison.

Thus the effects of intrinsic anharmonicity on the thermodynamic properties of mantle minerals may not be negligible, especially in the case of superadiabatic or hot regions of the mantle. These conclusions are, however, highly dependent upon the second-order parameters δ_T and q; significant improvement of our knowledge of these parameters is therefore required. Molecular dynamics simulations, which directly account for anharmonicity, are currently under progress in order to establish with more confidence the extent of anharmonic effects at high pressure. Moreover, in this study, we have only investigated the effects of anharmonicity on bulk thermodynamic properties: these results do not mean that anharmonicity does not exist at a microscopic level at high pressure and low temperature, even though most of vibrational properties of minerals can be described through the QHA. For intance, the a_i parameters are observed to differ from zero at room conditions were they have no noticeable effect on the heat capacity. Finally, anharmonicity will become important at the onset of phase transitions involving soft modes (e.g. possibly in $MgSiO_3$-perovskite) and will consequently affect properties such as the Gruneisen parameter, thermal expansion and heat capacity.

Acknowledgments. The authors wish to thank F. Guyot and S. C. Parker for fruitful comments and lively discussions, and A. Chopelas for providing data before publication. Careful comments from A. M. Hofmeister and an anonymous reviewer helped to improve the manuscript. This work has been supported by NERC grants GR3/6358 and GR3/6970.

REFERENCES

Akaogi, M., N. L. Ross, P. McMillan, and A. Navrotsky, The Mg_2SiO_4 polymorphs (olivine, modified spinel and spinel)-thermodynamic properties from oxide melt solution calorimetry, phase relations, and models of lattice vibrations, *Am. Mineral., 69*, 499-512, 1984.

Anderson, D. L., A seismic equation of state II, shear and thermodynamic properties of the lower mantle, *Phys. Earth Planet. Inter., 45*, 307-323, 1987.

Anderson, D. L., *Theory of the Earth*, Blackwell Scientific Publications, Oxford, 1989.

Anderson, O. L., and I. Suzuki, Anharmonicity of three minerals at high temperature: Forsterite, fayalite, and periclase, *J. Geophys. Res., 88*, 3549-3556, 1983.

Anderson, O. L. and S. Yamamoto, The interrelationship between thermodynamic properties obtained by the piston-cylinder high pressure experiments and RPR high temperature experiments for NaCl, in *High Pressure Research in Mineral Physics, Geophys. Monogr. Ser.*, vol. 39, edited by M. H. Manghnani and Y. Syono, pp. 289-298, AGU, Washington, D. C., 1987.

Besson, J. M., J. P. Pinceaux, C. Anastopoulos, and B. Velde, Raman spectra of olivine up to 65 kbars, *J. Geophys. Res., 87*, 10773-10775, 1982.

Boehler, R., Adiabats of quartz, coesite, olivine and magnesium oxide to 50 kbars and 1000K, and the adiabatic gradient in the Earth mantle, *J. Geophys. Res., 87*, 5501-5506, 1982.

Born, M., and K. Huang, *Dynamical Theory of Crystal Lattices*, Clarendon Press, Oxford, 1954.

Brown, J. M., M. D. Furnish, and R. G. McQueen, Thermodynamics for $(Mg,Fe)_2SiO_4$ from the Hugoniot, in *High Pressure Research in Mineral Physics, Geophys. Monogr. Ser.*, vol. 39, edited by M. H. Manghnani and Y. Syono, pp. 373-389, AGU, Washington, D. C., 1987.

Brown, M., and T. J. Shankland, Homogeneity and temperatures in the lower mantle, *Phys. Earth Planet. Inter., 38*, 51-58, 1985.

Catlow, C. R. A., and G. D. Price, Computer modelling of solid-state inorganic materials, *Nature, 347*, 243-248,1990.

Catti, M., Theoretical computation of physical properties of mantle minerals, in *Chemistry and Physics of Terrestrial Planets, Advances in Physical Geochemistry*, vol. 6, edited byS. K. Saxena, Springer Verlag, New York, pp. 224-250, 1986.

Chopelas, A., Thermal expansion, heat capacity, and entropy of MgO at mantle pressures, *Phys. Chem. Miner., 17*, 142-148, 1990a.

Chopelas, A., Thermochemical properties of forsterite at mantle pressures derived from vibrational spectroscopy, *Phys. Chem. Miner., 17*, 149-156, 1990b.

Chopelas, A., Thermodynamic parameters of solids at high pressure from vibrational spectroscopy : MgO and $MgAl_2O_4$, in *High Pressure Research*, vol.5, edited by W. B. Holzapfel and P. G. Johannsen, pp. 711-713, Gordon and Breach Science, New York, 1990c.

Chopelas, A., Single crystal Raman spectra of forsterite, fayalite and monticellite, *Am. Mineral., 76*, 1101-1109, 1991.

Cochran, W., *The Dynamics of Atoms in Crystals*, Edward Arnold, London, 1973.

Cohen, R. E., Calculation of elasticity and high pressure instabilities in corundum and stishovite with the potential induced breathing model, *Geophys. Res. Lett., 14*, 37-40, 1987.

Dietrich, P., and J. Arndt, Effects of pressure and temperature on the physical behavior of mantle-relevant olivine, orthopyroxene and garnet, II, Infrared absorption and Gruneisen parameters, in *High Pressure Researches in Geoscience*, edited by W. Schreyer, pp. 307-309, E. Schweizerbartsche, Stuggard, 1982.

Dovesi, R., C. Pisani, C. Roetti, and B. Silvi, The electronic structure of α-quartz: A periodic Hartree-Fock calculation, *J. Chem. Phys., 86*, 6967-6971, 1987.

Fiquet, G., Ph. Gillet, and P. Richet, Anharmonicity and high-temperature heat capacity of crystals: the examples of Ca_2GeO_4, Mg_2GeO_4 and $CaMgGeO_4$ olivines, *Phys. Chem. Minerals*, in press, 1992.

Gillet, Ph., J. M. Malézieux, and M. C. Dhamelincourt, MicroRaman-multichannel spectroscopy up to 2.5 GPa using a sapphire-anvil cell: Experimental setup and some applications, *Bull. Mineral., 111*, 1-15, 1988.

Gillet, Ph., F. Guyot, and J. M. Malézieux, High-pressure, high-teperature Raman spectroscopy of Ca_2GeO_4 (olivine form): Some insights on anharmonicity, *Phys. Earth Planet. Inter., 58*, 141-154, 1989.

Gillet, Ph., P. Richet, F. Guyot, and G. Fiquet, High temperature properties of forsterite, *J. Geophys. Res., 96*, 11805-11816, 1991.

Graham, E. K., and G. R. Barsch, Elastic constants of single-crystal forsterite as a function of temperature and pressure, *J. Geophys. Res., 74*, 5949-5960, 1969.

Gruneisen, E., Theorie des festen zustandes einatomiger elemete, *Ann. Phys., 39*, 257-306, 1912.

Hardy, J. R., Temperature and pressure dependence of intrinsic anharmonic and quantum corrections to the equation of state, *J. Geophys. Res., 85*, 7011-7015, 1980.

Hazen, R. M., Effect of temperature and pressure on the crystal structure of forsterite, *Am. Mineral., 61*, 1280-1293, 1976.

Hazen, R. M., and L. W. Finger, *Comparative Crystal Chemistry: Temperature, Pressure, Composition and the Variation of the Crystal Structure*, John Wiley, New York, 1982.

Hazen, R. M., and L. W. Finger, High-pressure crystal chemistry of andradite and pyrope: Revised procedures for high-pressure diffraction experiments, *Am. Mineral., 74*, 352-359, 1989.

Hemley, R. J., Pressure dependence of Raman spectra of SiO_2 polymorphs : α-quartz, coesite and stishovite, in *High Pressure Research in Mineral Physics, Geophys. Monogr. Ser.*, vol. 39, edited by M. H. Manghnani and Y. Syono, pp. 347-359, AGU, Washington, D. C., 1987.

Hofmeister, A. M., Single-crystal absorption and reflection infrared spectroscopy of forsterite and fayalite, *Phys. Chem. Miner., 14*, 499-513, 1987.

Hofmeister, A. M., J. Xu, H. K. Mao, P. M. Bell, and T. C. Hoering, Thermodynamics of Fe-Mg olivines at mantle pressure: Mid- and far-infrared at high pressure, *Am. Mineral., 74*, 281-306, 1989.

Iishi, K., Lattice dynamics of forsterite, *Am. Mineral., 63*, 1198-1208, 1978.

Isaak, D. G., O. L. Anderson, and T. Goto, Elasticity of single-crystal forsterite to 1700K, *J. Geophys. Res., 94*, 5895-5906, 1989.

Isaak, D. G., R. E. Cohen, and M. J. Mehl, Calculated elastic and thermal properties of MgO at high pressures and temperatures, *J. Geophys. Res., 95*, 7055-7067, 1990.

Kieffer, S. W., Thermodynamics and lattice vibrations of minerals, 1, Mineral heat capacities and their relationship with simple lattice vibrational modes, *Rev. Geophys. Space Phys., 17*, 1-19, 1979 a.

Kieffer, S. W., Thermodynamics and lattice vibrations of minerals, 2, Vibrational characteristics of silicates, *Rev. Geophys. Space Phys., 17*, 20-34, 1979 b.

Kieffer, S. W., Thermodynamics and lattice vibrations of minerals, 3, Lattice dynamics and an approximation for minerals with application to simple substances and framework silicates, *Rev. Geophys. Space Phys., 17*, 35-59, 1979 c.

Kieffer, S. W., Thermodynamics and lattice vibrations of minerals, 4, Application to chain and sheet and orthosilicates, *Rev. Geophys. Space Phys., 18*, 862-886, 1980.

Kieffer, S. W., Thermodynamics and lattice vibrations of minerals, 5, Applications to phase equilibria, isotopic fractionation, and high pressure thermodynamic properties, *Rev. Geophys. Space Phys., 20*, 827-849, 1982.

Kudoh, Y., and Y. Takeuchi, The crystal structure of forsterite Mg_2SiO_4 under pressure up to 149 kbars, *Z. Kristallogr., 171*, 291-302, 1985.

Kumazawa, M., and O. L. Anderson, Elastic moduli, pressure derivatives and temperature derivatives of single-crystal olivine and single-crystal forsterite, *J. Geophys. Res.*, 74, 5961-5972, 1969.

Lam, P. K., Y. Rici, M. W. Lee and S. K. Sharma, Structural distorsions and vibrational modes in Mg_2SiO_4, *Am. Mineral., 75*, 109-119, 1990.

Leibfried, G., and W. Ludwig, Theory of anharmonic effects in crystals, *Solid State Phys., 12*, 275-444, 1960.

Mammone, J. F., and S. K. Sharma, Pressure and temperature dependence of the Raman spectra of rutile-structure oxides, *Carnegie Inst. Washington Year Book, 78*, 369-373, 1979.

Matsui, T., and M. H. Manghnani, Thermal expansion of single-crystal forsterite to 1023K by Fizeau interferometry, *Phys. Chem. Miner., 12*, 201-210, 1985.

Parker, S. C., and G. D. Price, Computer modelling of phase transitions in minerals, in *Advances in Solid State Chemistry, 1*, pp. 295-327, edited by C. R. A. Catlow, JAI, London, 1989.

Price, G. D., S. C. Parker, and M. Leslie, The lattice dynamics of forsterite, *Mineral. Mag., 51*, 157-170, 1987a.

Price, G. D., S. C. Parker, and M. Leslie, The lattice dynamics and thermodynamics of the Mg_2SiO_4 polymorphs, *Phys. Chem. Miner., 15*, 181-190, 1987b.

Quareni, F., and F. Mulargia, The validity of common approximate expressions for the Gruneisen parameter, *Geophys. J. R. Astron. Soc., 93*, 505-519, 1988.

Quareni, F., and F. Mulargia, The Gruneisen parameter and adiabatic gradient in the Earth's interior, *Phys. Earth Planet. Inter., 55*, 221-233, 1989.

Rao, K. R., S. L. Chaplot, N. Choudhury, S. Ghose, J. M. Hastings, L. M. Corliss, and D. L. Price, Lattice dynamics and inelastic neutron scattering from forsterite, Mg_2SiO_4: Phonon dispersion relation, density of states and specific heat, *Phys. Chem. Miner., 16*, 83-97, 1988.

Reynard, B., Single-crystal infrared reflectivity of pure Mg_2SiO_4 forsterite and $(Mg_{0.86},Fe_{0.14})_2SiO_4$ olivine- New data and a reappraisal, *Phys. Chem. Miner., 18*, 19-25, 1991.

Richet, P., and G. Fiquet, High-temperature heat capacity and premelting of minerals in the system MgO-CaO-Al_2O_3-SiO_2, *J. Geophys. Res.*, 96, 445-456, 1991.

Robie, R. A., B. S. Hemingway, and H. Takei, Heat capacities and entropies of Mg_2SiO_4, Mn_2SiO_4, Co_2SiO_4 between 5 and 385 K, *Am. Mineral., 67*, 470-482, 1982.

Servoin, J. L., and B. Piriou, Infrared reflectivity and Raman scattering of Mg_2SiO_4 single-crystals. *Phys. Status Solidi, B55*, 677-686, 1973.

Sharma, S. K., Applications of advanced Raman spectroscopic techniques in Earth sciences, in *Raman Spectroscopy: Sixty Years on Vibrational Spectra and Structure*, vol 17B, edited by H. D. Bist et al., pp. 513-568, Elsevier Science, New York, 1989.

Stacey, F. D., A thermal model of the Earth, *Phys. Earth Planet. Inter., 15*, 341-348, 1977.

Suzuki, I., Thermal expansion of periclase and olivine and their anharmonic properties, *J. Phys. Earth, 23*, 145-159, 1975.

Suzuki, , I., O. L. Anderson, and Y. Sumino, Elastic properties of a single-crystal forsterite Mg_2SiO_4, up to 1200 K, *Phys. Chem. Miner., 10*, 38-46, 1983.

Syono, Y., and T. Goto, Behavior of single-crystal forsterite under dynamic compression, in *High Pressure Research in Geophysics*, edited by S. Akimoto and M. H. Manghnani, pp. 563-578, Center for Academic Pulblications, Tokyo, 1982.

Takeuchi, Y., Y. Takamitsu, N. Haga, and M. Hirano, High-temperature crystallography of olivines and spinels, in *Material Science of the Earth Interior*, edited by I. Sunagawa, pp. 191-231, Terrapub, Tokyo, 1984.

Webb, S. L., The elasticity of the upper mantle orthosilicates olivine and garnet up to 3 GPa, *Phys. Chem. Miner., 16*, 684-692, 1989.

White, G. K., R. B. Roberts, and J. G. Collins, Thermal properties and Gruneisen functions of forsterite, Mg_2SiO_4, *High Temp. High Pressures*, 17, 61-66, 1985.

Wolf, G. H., and M. S. T. Bukowinski, Theoretical study of the structural properties and equations of state of $MgSiO_3$ and $CaSiO_3$ perovskites : implications for the lower mantle composition, in *High Pressure Research in Mineral Physics, Geophys. Monogr. Ser.*, vol. 39, edited by M. H. Manghnani and Y. Syono, pp. 313-331, AGU, Washington, D. C., 1987.

P. Gillet, Laboratoire de Géologie, Ecole Normale Supérieure de Lyon, 46 Allée d'Italie, 69364 Lyon Cédex 07, France.

G. D. Price, Department of Geological Sciences, University College London, Gower Street, WC1 E 6BT London, England.

B. Reynard, Laboratoire de Minéralogie Physique, Géosciences Rennes, Université de Rennes I, 35042 Rennes Cedex, France.

(Received March 20, 1991;
revised May 12, 1992;
accepted June 12, 1992.)